

Significant enhancement of crystallization kinetics of polylactide in its immiscible blends through an interfacial effect from comb-like grafted side chains

Yin Chen¹, Yaqiong Zhang^{1*}, Feng Jiang¹, Junyang Wang¹, Zhaohua Xu² & Zhigang Wang^{1*}

¹CAS Key Laboratory of Soft Matter Chemistry; Hefei National Laboratory for Physical Sciences at the Microscale; Department of Polymer Science and Engineering, University of Science and Technology of China, Hefei 230026, China

²Department of Material Technology, Jiangmen Polytechnic, Jiangmen 529090, China

Received August 15, 2015; accepted September 30, 2015; published online January 21, 2016

A significant enhancement in isothermal crystallization kinetics of biodegradable polylactide (PLA) in its immiscible blends can be accomplished through blending it with a comb-like copolymer. PLA was blended with poly(ethylene glycol) methyl ether acrylate (PEGA) and poly[poly(ethylene glycol) methyl ether acrylate] (PPEGA, a comb-like copolymer), respectively. The results measured from phase contrast optical microscopy (PCOM) and differential scanning calorimetry (DSC) indicate that PLA and PEGA components are miscible, whereas PLA and PPEGA components are immiscible. The study of crystallization kinetics for PLA/PEGA and PLA/PPEGA blends by means of polarized optical microscopy (POM) and DSC indicates that both PEGA and PPEGA significantly increase the PLA spherulitic growth rates, G , although PLA/PPEGA blends are immiscible and the glass transition temperatures of PLA only have slight decreases. PPEGA component enhances nucleation for PLA crystallization as compared with PEGA component owing to the heterogeneous nucleation effect of PPEGA at the low composition of 20 wt%, while PLA crystallization-induced phase separation for PLA/PEGA blend might cause further nucleation at the high composition of 50 wt%. DSC measurement further demonstrates that isothermal crystallization kinetics can be relatively more enhanced for PLA/PPEGA blends than for PLA/PEGA blends. The “abnormal” enhancement in G for PLA in its immiscible blends can be explained by local interfacial interactions through the densely grafted PEGA side chains in the comb-like PPEGA, even though the whole blend system (PLA/PPEGA blends) represents an immiscible one.

biodegradable polymer, spherulite, growth rate, phase separation, nucleation

Citation: Chen Y, Zhang YQ, Jiang F, Wang JY, Xu ZH, Wang ZG. Significant enhancement of crystallization kinetics of polylactide in its immiscible blends through an interfacial effect from comb-like grafted side chains. *Sci China Chem*, 2016, 59: 609–618, doi: 10.1007/s11426-015-5515-6

1 Introduction

Polymers for their thermoformability, weight savings and low costs have taken the place of metals in many fields, such as cars, buildings, and roads. However, with increasing environmental concerns and cost rises for petroleum-based polymers, biodegradable polymers have attracted increasing

interest for their excellent performances in renewability, biodegradability and biocompatibility [1–4]. Polylactide (PLA) is one of the most promising biopolymers [5–7]. However, poor thermal resistance, slow crystallization rate and low dimensional stability of PLA restrict its practical applications [8]. Various approaches have been adopted to improve the crystallization kinetics of PLA, such as blending, copolymerization and surface coating [9–14], among which blending is the most economic and effective method [15].

*Corresponding authors (email: zhangyaq@mail.ustc.edu.cn; zgwang2@ustc.edu.cn)

Because miscibility in polymer blends is crucial to the design of new polymeric materials with desired applicable properties, the relationships between miscibility and crystallization kinetics in polymer blends have attracted much attention in both academic and industrial fields [16–20]. Miscibility in polymer blends shows significant influences on crystallization kinetics of semicrystalline polymer components in various blends [21]. In a limited number of polymer blends, the glass transition temperature (T_g) of the amorphous polymer component (in the experimental temperature range) is lower than that of the crystallizable polymer component, and then the T_g of the blends decreases with increasing composition of the lower T_g polymer component. In this case, at certain crystallization temperatures the chain mobility of the crystallizable component in the blends is higher than in neat homopolymer, which facilitates the chain motion in the melt towards the growing crystal fronts and the further arrangement of the otherwise stiff chains into the crystals, providing a positive contribution to the spherulitic growth rate. For the blends of PLA mixed with low T_g components, such as PLA/poly(ethylene oxide) (PLA/PEO) [13,14,22,23], and PLA/poly(ethylene glycol) (PLA/PEG) blends [19,24,25], the T_g 's of the blends are lower than that of neat PLA, and the spherulitic growth rate increases with increasing composition of the lower T_g polymers.

On the other hand, for the partially miscible or immiscible polymer blends the amorphous component can be segregated as a dispersed phase. The separated phase domains are composed of neat amorphous polymer if the components are immiscible, or may contain small amounts of the crystallizable polymer if some degrees of miscibility exist. In a number of polymer blends, the effect of an immiscible component on the spherulitic growth rate has been experimentally measured. For some blends the addition of an immiscible polymer causes decrease in spherulitic growth rate, as measured in isotactic polypropylene/poly(dicyclohexylitaconate) (iPP/PDCHI) [26], poly(3-hydroxybutyrate)/poly(methylene oxide) (P3HB/POM) [27], isotactic polypropylene/ethylene-propylene rubber (iPP/EPR) blends [28,29], whereas for some other immiscible blend systems no effects of the amorphous components on the spherulitic growth rate have been found, as measured in P3HB/EPR [30], PEO/PDCHI [21,31], PEO/plasticized poly(vinyl chloride) (PEO/PVC) [32], iPP/poly(vinyl butyral) (iPP/PVB) blends [33], and PLA/poly(ϵ -caprolactone) (PLA/PCL) blends [34].

On the basis of the available knowledge from the literature, we raise a fundamental question in this study, can the spherulitic growth rates for semicrystalline polymers in immiscible blends be significantly enhanced through the local interfacial interactions at the phase domain boundary? For answering this question, two types of polymer blends with obviously contrast miscibility, polylactide/poly(ethylene glycol) methyl ether acrylate (PLA/PEGA) blends and polylactide/poly[poly(ethylene glycol) methyl ether acrylate]

(PLA/PPEGA) blends were prepared respectively to investigate the variations in crystallization kinetics of PLA component in these blends, including both the nucleation rate and spherulitic growth rate. The isothermal crystallization kinetics of PLA component in PLA/PEGA and PLA/PPEGA blends in a wide temperature range were measured by applying polarized optical microscopy (POM) and differential scanning calorimetry (DSC). It is surprising to find that the spherulitic growth rates of PLA in PLA/PPEGA blends can be significantly enhanced as well as in PLA/PEGA blends, even though PLA/PPEGA blends represent an immiscible blend system. In addition, PPEGA can provide an obvious nucleation effect for PLA crystallization in the blends. The mechanism for the above observed unique and abnormal phenomena is provided in this article.

2 Experimental

2.1 Materials

Poly(*L*-lactide) (PLA, sample code PLA4032D) used in this study was purchased from NatureWorks China/Hong Kong, Shanghai, China. It had a weight-average molecular mass, M_w of 1.8×10^5 g/mol and a polydispersity index of 1.5. PLA was used after drying under vacuum at 60 °C for 24 h. Poly(ethylene glycol) methyl ether acrylate (>99.5%, PEGA with monomethyl terminated with eight ethylene glycol repeat units, and the number-average molecular mass, M_n of 480 g/mol) was purchased from the Sigma-Aldrich Company (USA). Synthesis of poly[poly(ethylene glycol) methyl ether acrylate] (PPEGA) comb-like copolymer can be found in our recent work [35]. PPEGA had the number-average molecular mass (M_n) of 4680 g/mol and the weight-average molecular mass (M_w) of 6100 g/mol. PEGA and PPEGA were dried under vacuum at 35 °C for 24 h prior to use. The melting points of PEGA and PPEGA were -0.5 and -2.5 °C, respectively, and both were below the room temperature. Therefore, at the experimental isothermal crystallization temperatures applied in this study both PEGA and PPEGA were in the amorphous state.

2.2 Preparation of PLA/PEGA and PLA/PPEGA blends

The thin film samples were used for polarized optical microscope observation. The preparation procedure for PLA/PEGA blend films is described as follows. PEGA and PLA components with certain mass compositions were dissolved in common solvent, chloroform to form 5.0 wt% solutions. The solutions were stirred at room temperature for 12 h, and then were cast on cover glasses. When chloroform was evaporated, PLA/PEGA blend films formed on cover glasses, which were further dried under vacuum to constant masses. The preparation procedure for PLA/PPEGA blend

films is different from that for the preparation of PLA/PGEA blend films because of immiscibility between PLA and PGEA components. The PGEA and PLA components with certain mass compositions were dissolved in chloroform to form 5.0 wt% solutions, respectively, and the solutions were stirred at room temperature for 5 h. Afterwards the PGEA solution was added into the PLA solution with further stirring for 7 h to form the PLA/PGEA solutions, which were cast on cover glasses to form PLA/PGEA blend films. The blend film thicknesses were about 20 μm .

The PLA/PGEA 80/20 and PLA/PGEA 50/50 blend samples for DSC measurements were prepared according to the following procedure. The PLA and PGEA components were dissolved in chloroform to form the solutions. After stirring for 12 h, the solutions were poured into Petri dishes, chloroform was allowed to evaporate, and then the obtained PLA/PGEA blend samples were dried under vacuum at 35 $^{\circ}\text{C}$ to constant masses. Because of immiscibility between PLA and PGEA, the PLA/PGEA 80/20 and PLA/PGEA 50/50 blend samples for DSC measurements were prepared using the solution co-precipitation method. The PLA and PGEA components were mixed in chloroform to form solutions, which were poured into a large amount of cold diethyl ether under vigorous stirring to precipitate PLA/PGEA blends. After being washed for two times with diethyl ether, the obtained PLA/PGEA blends were dried under vacuum at 35 $^{\circ}\text{C}$ to constant masses.

2.3 Nucleation and growth of spherulites observed by polarized optical microscope

The nucleation and growth of PLA spherulites for the film samples of PLA/PGEA and PLA/PGEA blends during isothermal crystallization in a wide temperature range were observed by using a polarized optical microscopy (POM, Olympus BX53, Japan) equipped with a CCD camera (MicroPublisher 3.3 RTV). The prepared PLA/PGEA and PLA/PGEA blend film samples were held at 200 $^{\circ}\text{C}$ for 5 min to erase previous thermal histories in one hot stage, and then were transferred to another hot stage set at certain crystallization temperatures below the nominal melting point of PLA for isothermal crystallization. The polarized optical micrographs were recorded at appropriate time intervals depending on the spherulitic growth rates of the film samples. The average radial growth rates of PLA spherulites, G were obtained from the slopes of changes of spherulite radius with crystallization time.

2.4 Isothermal crystallization kinetics measured by differential scanning calorimeter

DSC heat flow curves for PLA/PGEA and PLA/PGEA blend samples sealed in aluminum pans were recorded by using a TA Q2000 DSC (TA Instruments, USA). The iso-

thermal crystallization kinetics for PLA/PGEA and PLA/PGEA blend samples were evaluated using DSC by melting the samples at 200 $^{\circ}\text{C}$ for 5 min to eliminate thermal histories, rapidly cooling the melts at a cooling rate of 50 $^{\circ}\text{C}/\text{min}$ to the crystallization temperatures, and then holding these samples at these temperatures for 60 min to allow completion of crystallization from the quiescent melts. Finally, the crystallized blend samples were heated again with a heating rate of 10 $^{\circ}\text{C}/\text{min}$ to 200 $^{\circ}\text{C}$ to measure the melting points. Measurements of T_g were performed according to the following procedure. The blend samples were first melted at 200 $^{\circ}\text{C}$ for 5 min to erase previous thermal histories followed by quenching to -90 $^{\circ}\text{C}$ at a cooling rate of 50 $^{\circ}\text{C}/\text{min}$, and then DSC heating scans were run at a heating rate of 10 $^{\circ}\text{C}/\text{min}$, from which the T_g values were evaluated.

3 Results and discussion

3.1 Miscibility evaluation for PLA/PGEA and PLA/PGEA blends

The miscibility between polymer components plays a key role in changing the crystallization kinetics of polymer blends [18,36]. In our previous work, PLA and PGEA components are confirmed to be immiscible by phase contrast optical microscope observation and DSC measurements [35]. The miscibility between PLA and PGEA components needs an evaluation. Figure 1 shows phase contrast optical micrographs for PLA/PGEA 80/20, PLA/PGEA 50/50, PLA/PGEA 80/20 and PLA/PGEA 50/50 blends as observed at 200 $^{\circ}\text{C}$. The featureless phase morphology for PLA/PGEA 80/20 and PLA/PGEA 50/50 blends clearly indicates the miscibility between PLA and PGEA components. The phase separation behavior for PLA/PGEA blends is worthy of further study, which is out of the scope of this work [24]. Whereas, an obvious phase separation can be seen in PLA/PGEA 80/20 and PLA/PGEA 50/50 blends, clearly indicating immiscibility between PLA and PGEA components.

The changes of T_g of PLA in the blends with PGEA or PGEA composition were measured by using DSC, which could be further used to evaluate the miscibility in the blends. Heat capacity, C_p curves and temperature derivative heat capacity curves for PLA/PGEA blends with PGEA compositions of 0 wt%, 1 wt%, 5 wt%, 10 wt%, 15 wt%, and 20 wt% are shown in Figure S1 (Supporting Information online), from which the T_g can be obtained. Figure 2 shows the changes of T_g with PGEA or PGEA composition for PLA/PGEA and PLA/PGEA blends. The solid curve is the fitted line by applying the Fox equation for PLA/PGEA blends. It is easily found that the change of T_g for PLA component with PGEA composition in the blends follows the prediction by the Fox equation. The obvious

accord of the measured T_g values with the Fox equation indicates that PEGA component is miscible with PLA component in the blends. In conclusion, PLA and PEGA components are miscible, whereas PLA and PPEGA components are immiscible. PLA/PEGA and PLA/PPEGA blends are nicely comparable blend systems for an investigation on the miscibility effects on the nucleation and growth of PLA spherulites in the blends during isothermal crystallization.

3.2 Equilibrium melting temperatures for PLA/PEGA and PLA/PPEGA blends

For study on crystallization kinetics of polymer blends, the equilibrium melting temperature (T_m^0) is a crucial parameter, which can be obtained by applying the Hoffman-Weeks method [37,38]. Figure 3 shows the changes of melting temperature (T_m) as functions of isothermal crystallization temperature (T_c) for PLA/PEGA 50/50, PLA/PPEGA 50/50, PLA/PEGA 80/20 and PLA/PPEGA 80/20 blends. The T_m values are taken from the heating scan curves for the crystallized blend samples at a heating rate of 10 °C/min (Figures S2–S6). Note that two melting peaks can be observed for some heating scan curves. The low temperature melting peak, T_{m1} , is taken to measure T_m^0 because the high temperature melting peak, T_{m2} , is related to the melting-recrystallization-melting mechanism [39,40]. It can be found that the melting temperatures of PLA/PEGA or PLA/PPEGA blends increase with increasing crystallization temperature, indicating improvement of crystal perfection for PLA with increasing crystallization temperature. The T_m^0 values for PLA/PEGA and PLA/PPEGA blends can be obtained by extrapolating the data points to the $T_m=T_c$ line. The T_m^0 values for PLA/PPEGA 50/50 blend are higher than that for PLA/PEGA 50/50 blend as shown in Figure 3(a), and similarly the T_m^0 value for PLA/PPEGA 80/20 blend is higher than that for PLA/PEGA 80/20 blend as shown in Figure 3(b). The T_m^0 values for PLA in neat PLA, PLA/PEGA 80/20, PLA/PEGA 50/50, PLA/PPEGA 80/20 and PLA/PPEGA 50/50 blend samples are listed in Table 1. The change of T_m as a function of T_c for neat PLA can be found in Figure S7. Comparing the T_m^0 values of PLA/PPEGA blends with that of PLA/PEGA blends, one finds obviously less melting point depression for the former than for the latter, indicating the difference in miscibility for these two blend systems. The above result is consistent with that shown in Figures 1 and 2, that is to say, PLA/PEGA blends represent a miscible one, while PLA/PPEGA blends represent an immiscible one.

3.3 Nucleation and spherulitic growth for PLA/PEGA 50/50 and PLA/PPEGA 50/50 blend films

The crystalline morphological evolutions for PLA/PEGA 50/50 and PLA/PPEGA 50/50 blend films during isothermal

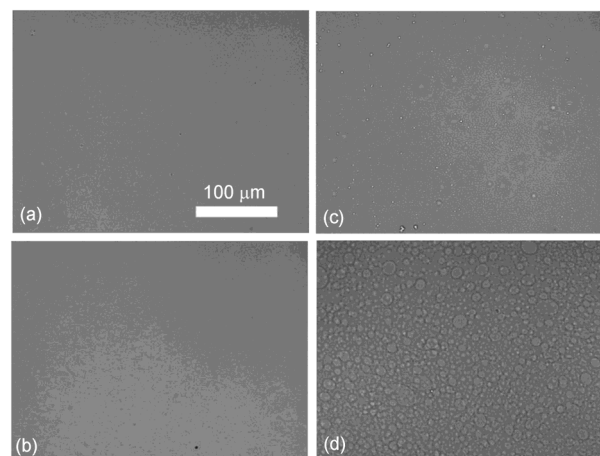


Figure 1 Phase contrast optical micrographs for (a) PLA/PEGA 80/20 blend, (b) PLA/PEGA 50/50 blend, (c) PLA/PPEGA 80/20 blend and (d) PLA/PPEGA 50/50 blend. The scale bar in (a) represents 100 μm and is applied to all other micrographs. The micrographs were taken when the samples were melted at 200 °C (color online).

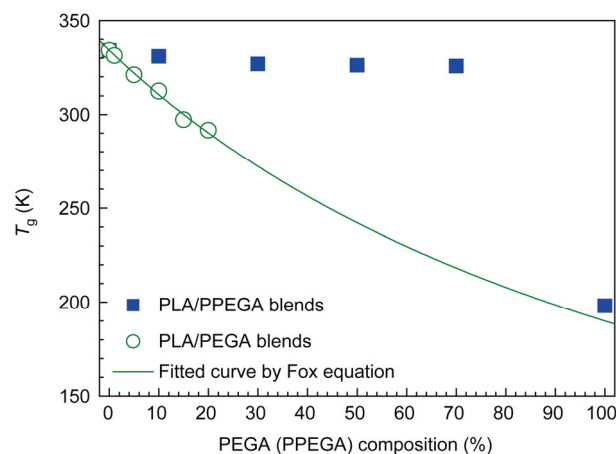


Figure 2 Changes of glass transition temperature (T_g) with PEGA or PPEGA composition for PLA/PEGA and PLA/PPEGA blends. The solid olive curve is the fitted line by applying the Fox equation for PLA/PEGA blends.

crystallization were observed by using polarized optical microscope. Figures 4 and 5 show the nucleation and spherulitic growth for PLA/PEGA 50/50 and PLA/PPEGA 50/50 blend films during isothermal crystallization at different temperatures, respectively. It can be seen that for both blend systems the nucleus number for PLA crystallization decreases with increasing crystallization temperature due to the decreasing undercooling degree. Meanwhile, the impingement time for the growing spherulites becomes shortened with decreasing crystallization temperature due to increasing spherulitic growth rate. One obvious difference is that the formation of ring-banded spherulites for PLA/PEGA 50/50 blend films occurs at T_c of 90, 100 and 110 °C, while for PLA/PPEGA 50/50 blend films it occurs at higher T_c of 100, 110 and 120 °C. The ring bands for PLA/PPEGA

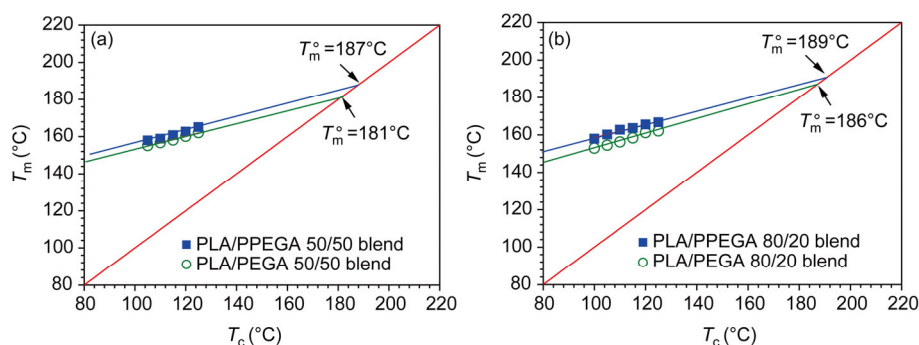


Figure 3 Changes of melting temperature (T_m) as functions of isothermal crystallization temperature (T_c) for (a) PLA/PEGA 50/50 and PLA/PPEGA 50/50 blend samples, and (b) PLA/PEGA 80/20 and PLA/PPEGA 80/20 blend samples. The red lines indicate the equilibrium lines given by $T_m = T_c$, and the olive and blue lines represent linear regressions.

Table 1 Equilibrium melting temperature (T_m^0) for PLA in neat PLA, PLA/PEGA 80/20, PLA/PEGA 50/50, PLA/PPEGA 80/20 and PLA/PPEGA 50/50 blends

Sample code	T_m^0 (°C)
neat PLA	192
PLA/PEGA 80/20 blend	186
PLA/PEGA 50/50 blend	181
PLA/PPEGA 80/20 blend	189
PLA/PPEGA 50/50 blend	187

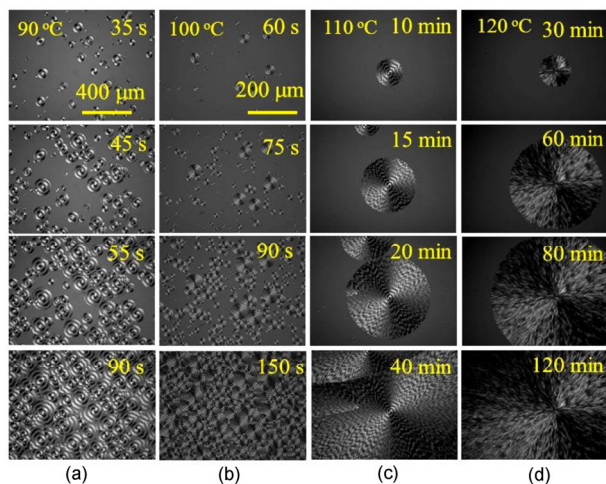


Figure 4 Selected POM micrographs for PLA/PEGA 50/50 blend films during isothermal crystallization at (a) 90 °C, (b) 100 °C, (c) 110 °C and (d) 120 °C. The scale bar in the top micrograph of (a) represents 400 μm and is applied to all the micrographs for (a), and the scale bar in the top micrograph of (b) represents 200 μm and is applied to all the micrographs for (b–d).

50/50 blend films are more regular than that for PLA/PEGA 50/50 blend films. This result is thought to be related to the higher T_m^0 value for PLA/PPEGA 50/50 blend, which requests higher crystallization temperatures for the same undercooling degrees.

Furthermore, at low T_c the impingement time for the growing spherulites in PLA/PPEGA 50/50 blend films is close to that in PLA/PEGA 50/50 blend films, while at high T_c the impingement time for the former is shorter than for

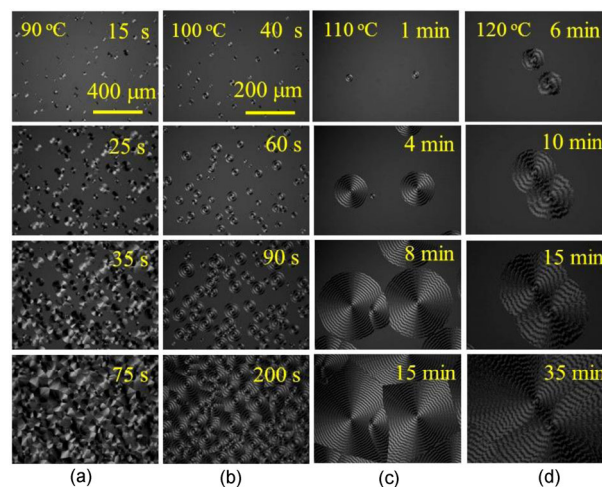


Figure 5 Selected POM micrographs for PLA/PPEGA 50/50 blend films during isothermal crystallization at (a) 90 °C, (b) 100 °C, (c) 110 °C and (d) 120 °C. The scale bar in the top micrograph of (a) represents 400 μm and is applied to all the micrographs for (a), and the scale bar in the top micrograph of (b) represents 200 μm and is applied to all the micrographs for (b–d).

the latter. For example, the impingement time is about 120 min at 120 °C and 90 s at 90 °C for PLA/PEGA 50/50 blend films, while the impingement time is 35 min at 120 °C and 75 s at 90 °C for PLA/PPEGA 50/50 blend films. Therefore, the nucleation densities and spherulitic growth rates need to be evaluated for further comparisons.

Figure 6 shows the changes of spherulite radius as functions of time for PLA/PEGA 50/50 and PLA/PPEGA 50/50 blend films during isothermal crystallization at T_c of 90 and 120 °C, respectively. It can be found that PLA spherulites all grow linearly with time and the spherulitic growth rates can be obtained from the slopes of the linearly fitted lines. At 90 °C the spherulitic growth rate for PLA/PEGA 50/50 blend film is higher than that for PLA/PPEGA 50/50 blend film (Figure 6(a)), while at 120 °C the spherulitic growth rate for PLA/PEGA 50/50 blend film is lower than that for PLA/PPEGA 50/50 blend film (Figure 6(b)). Note that the linearly fitted lines for PLA/PPEGA 50/50 blend films point

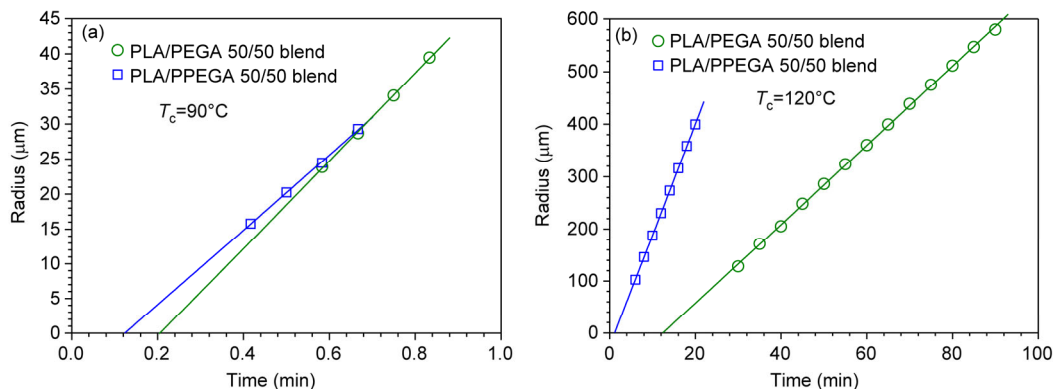


Figure 6 Changes of spherulite radius as functions of time for PLA/PEGA 50/50 and PLA/PPEGA 50/50 blend films during isothermal crystallization at T_c of (a) 90°C and (b) 120°C .

at the time on the x -axis much earlier than for PLA/PEGA 50/50 blend films, which indicates that the induction time of nucleation for PLA/PPEGA 50/50 blend films is shorter than for PLA/PEGA 50/50 blend films at the same crystallization temperature.

Figure 7 shows the changes of spherulitic growth rate as functions of undercooling ($T_m^0 - T_c$) for neat PLA, PLA/PEGA 50/50 and PLA/PPEGA 50/50 blend films. One can clearly see that the spherulitic growth rates for PLA/PEGA 50/50 and PLA/PPEGA 50/50 blend films are much higher than that for neat PLA. When comparing the result for PLA/PEGA 50/50 blend films with that for PLA/PPEGA 50/50 blend films, a turning point can be seen at the undercooling of 80°C , below which the spherulitic growth rates for PLA/PEGA 50/50 blend are close to that for PLA/PPEGA 50/50 blend, while above which the spherulitic growth rates for PLA/PEGA 50/50 blend are relatively higher than that for PLA/PPEGA 50/50 blend. Recalling that PLA/PEGA 50/50 blend is miscible, while PLA/PPEGA 50/50 blend is immiscible, the above result can be understood because PEGA component can decrease T_g for PLA component than PPEGA component in the blends (Figure 2). The result in Figure 7 indicates that although the T_g measurements show that PPEGA component added into PLA component does not decrease T_g of PLA component, the spherulitic growth rates for PLA component can still be significantly enhanced by PPEGA component as compared with neat PLA. This phenomenon looks unreasonable according to the previous reports [41–43], in which the liquid-liquid phase separation can induce nucleation for crystallization, but cannot enhance the spherulitic growth rates. Herein, we tentatively propose that for PLA/PPEGA 50/50 blend the densely grafted PEGA chains on the backbone chain of PPEGA (a comb-like copolymer) might simultaneously function together to enhance the chain segmental mobility of PLA chains through local interfacial interactions, which significantly enhances the formation of chain folding lamellae for PLA crystals, and thus increase the spherulitic growth rate.

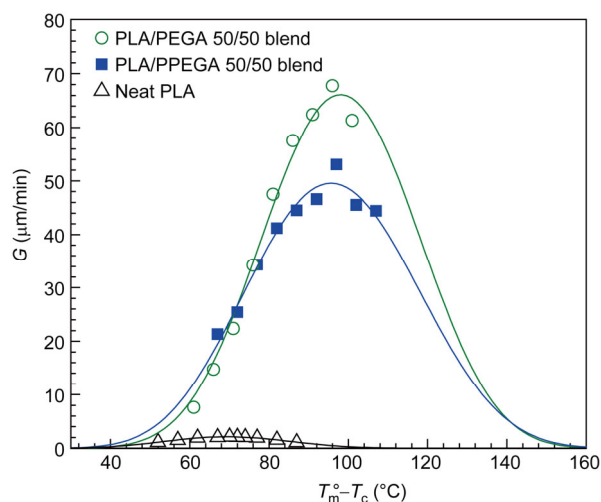


Figure 7 Changes of spherulitic growth rate as functions of undercooling ($T_m^0 - T_c$) for neat PLA, PLA/PEGA 50/50 and PLA/PPEGA 50/50 blend films. The solid lines represent the curves fitted with the data points on the basis of the Lauritzen-Hoffman growth theory.

In the above section, it has been shown that PPEGA can significantly enhance the spherulitic growth rates for PLA in the blend during isothermal crystallization. On the other hand, the nucleation effect of PPEGA component needs to be further evaluated. Figure 8 shows the changes of nucleation density, N_v , as functions of undercooling, $T_m^0 - T_c$ for PLA/PEGA 50/50 and PLA/PPEGA 50/50 blend films. The nucleation densities can be measured from the obtained POM micrographs [44]. Surprisingly, a turning point at the undercooling of 95°C is also observed, below which the nucleation densities for PLA/PEGA 50/50 blend are close to that for PLA/PPEGA 50/50 blend, while above which the nucleation densities for PLA/PEGA 50/50 blend are higher than that for PLA/PPEGA 50/50 blend. This result can be attributed to the difference in miscibility for these two blend systems. PLA and PPEGA are immiscible in PLA/PPEGA 50/50 blend. Thus, the crystal nuclei might form at the interfaces between PPEGA and PLA phases. This nucleation

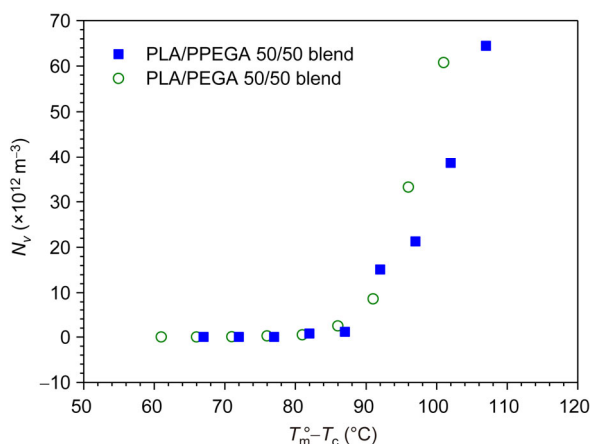


Figure 8 Changes of nucleation density (N_v) as functions of undercooling, $T_m^0 - T_c$ for PLA/PEGA 50/50 and PLA/PPEGA 50/50 blend films.

is caused by the decrease in surface free energy for the formation of crystal nuclei due to the presence of phase boundary [34,43,45]. We note that the crystal nuclei form at the beginning of isothermal crystallization for PLA/PPEGA 50/50 blend, and the number of nuclei keeps about constant during the whole isothermal crystallization process for each crystallization temperature. However, the number of nuclei shows some increases with crystallization time for each crystallization temperature for PLA/PEGA 50/50 blend, because PLA and PEGA are miscible in PLA/PEGA 50/50 blend and PLA crystallization can induce phase separation, which in turn enhances further nucleation [46–48].

3.4 Nucleation and spherulitic growth for PLA/PEGA 80/20 and PLA/PPEGA 80/20 blend films

To further confirm that PPEGA component can indeed enhance PLA crystallization kinetics, the nucleation and spherulitic growth of PLA component for PLA/PEGA 80/20 and PLA/PPEGA 80/20 blend films were observed by using POM (Figures S8 and S9). Figure 9 shows the changes of spherulite radius as functions of time for these two blend films during isothermal crystallization at T_c of 100 and 120 °C, respectively. All the plots show linear relationship

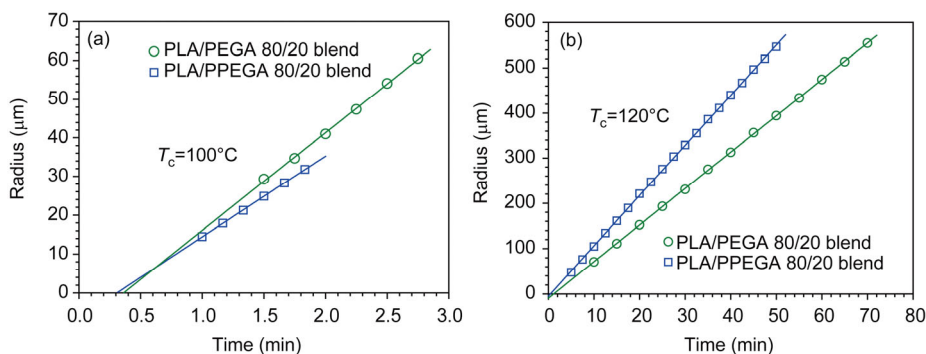


Figure 9 Changes of spherulite radius as functions of time for PLA/PEGA 80/20 and PLA/PPEGA 80/20 blend films during isothermal crystallization at T_c of (a) 100 °C and (b) 120 °C.

for the changes of spherulite radius as functions of time, similar to that for PLA/PEGA 50/50 and PLA/PPEGA 50/50 blend films.

Figure 10 shows the changes of spherulitic growth rate as functions of undercooling, $T_m^0 - T_c$ for PLA/PEGA 80/20 and PLA/PPEGA 80/20 blend films. Comparing with the results for 50/50 blend films shown in Figure 7, PEGA and PPEGA components at the composition of 20 wt% can also enhance the spherulitic growth rates, nevertheless behave less significantly than at the composition of 50 wt%. The change of spherulitic growth rate with undercooling ($T_m^0 - T_c$) for PLA/PPEGA 80/20 blend films is relatively broader than that for PLA/PEGA 80/20 blend films. At above the undercooling of 80 °C and below the undercooling of 95 °C the spherulitic growth rates for PLA/PEGA 80/20 blend are relatively higher than that for PLA/PPEGA 80/20 blend. At the other undercoolings the difference between these two blend systems is marginal. Overall, it can be concluded that although behaving immiscible with PLA component PPEGA component can indeed enhance the PLA spherulitic growth rate.

The nucleation densities for PLA/PEGA 80/20 and PLA/PPEGA 80/20 blend films are further evaluated. Figure 11 shows the changes of nucleation density (N_v) as functions of undercooling ($T_m^0 - T_c$) for PLA/PEGA 80/20 and PLA/PPEGA 80/20 blend films. The changing trend in Figure 11 looks different from that in Figure 8. A turning point at the undercooling of 90 °C is observed, below which the nucleation densities for PLA/PEGA 80/20 blend are close to that for PLA/PPEGA 80/20 blend, while above which the nucleation densities for PLA/PPEGA 80/20 blend are higher than that for PLA/PEGA 80/20 blend. This result can be also attributed to the difference in miscibility for these two blend systems. However, due to the lower PEGA composition in the blend (20 wt%) phase separation might not be induced by PLA crystallization. Thus, nucleation becomes less significant for PLA/PEGA 80/20 blend than for PLA/PPEGA 80/20 blend [46–48]. Note that the nucleation density values are relatively higher at 20 wt% than at 50 wt% PPEGA (or PEGA) compositions because of higher undercooling degree for the former than for the latter.

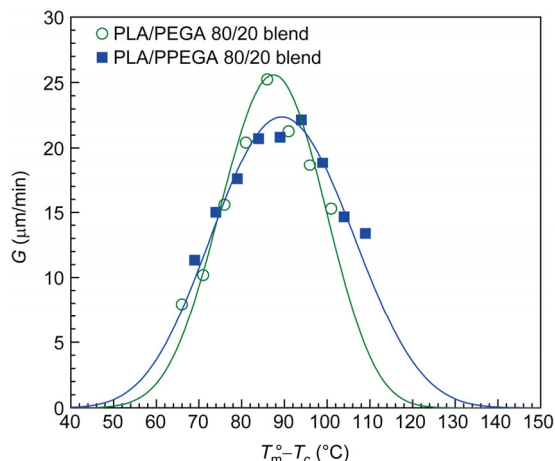


Figure 10 Changes of spherulitic growth rate as functions of undercooling ($T_m^\circ - T_c$) for PLA/PEGA 80/20 and PLA/PPEGA 80/20 blend films. The solid lines represent the curves fitted with the data points on the basis of the Lauritzen-Hoffman growth theory.

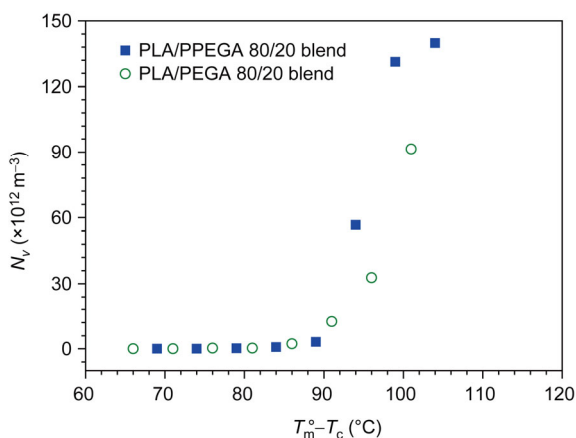


Figure 11 Changes of nucleation density (N_v) as functions of undercooling ($T_m^\circ - T_c$) for PLA/PEGA 80/20 and PLA/PPEGA 80/20 blend films.

3.5 Crystallization kinetics measured by DSC for PLA/PEGA and PLA/PPEGA blends

To provide further evidences for enhancements in crystallization kinetics the isothermal crystallization from melts for neat PLA, PLA/PEGA 80/20, PLA/PEGA 50/50, PLA/PPEGA 80/20 and PLA/PPEGA 50/50 blend samples was measured at different temperatures by using DSC. Figure 12 shows the heat flow curves for the above mentioned blend samples during isothermal crystallization at T_c of 120 °C. The heat flow curves for the above blend samples during isothermal crystallization at various temperatures are shown in Figures S10–S14. Note that these temperatures (above 100 °C) are located in the low undercooling range shown in Figures 7 and 10. The typical feature that can be immediately caught from Figure 12 is that the peak times of the exothermic peaks for PLA/PPEGA blends are shorter than that for PLA/PEGA blends. This implies that the isothermal

crystallization of PLA in the blends can be more enhanced through addition of PPEGA than PEGA at T_c of 120 °C. The other typical feature is that the isothermal crystallization rate of PLA/PPEGA blends (or PLA/PEGA blends) increases with increasing PPEGA (or PEGA) composition. The above result indicates that PPEGA (or PEGA) component in the blends can indeed enhance the spherulitic growth rates of PLA because PPEGA (or PEGA) component can increase the chain segmental mobility of PLA component.

To indicate the crystallization rate as measured by DSC, the crystallization half-time ($t_{1/2}$) is defined as the time at which the extent of crystallization reaches the half-value of relative crystallinity [45,49,50]. Figure 13 shows the changes of $t_{1/2}$ as functions of undercooling, $T_m^\circ - T_c$ for neat PLA, PLA/PEGA 50/50, PLA/PPEGA 50/50, PLA/PEGA 80/20 and PLA/PPEGA 80/20 blend samples. The results in Figure 13 indicate that the $t_{1/2}$ values for PLA/PPEGA and PLA/PEGA blends are much lower than that for neat PLA sample and the $t_{1/2}$ values for PLA/PPEGA blends are lower than that for PLA/PEGA blends at the same undercooling degrees. The DSC measurements demonstrate that at the isothermal temperatures above 100 °C, the immiscible PPEGA component can truly more significantly enhance the crystallization kinetics of PLA in the blends than the miscible PEGA component.

All the above results show that PPEGA component can significantly enhance the PLA crystallization rate in PLA/PPEGA blends through increasing the nucleation density and spherulitic growth rate. Figure 14 provides a schematic illustration for the related mechanism. Due to immiscibility, PPEGA phase domains are dispersed in the PLA matrix as individual phases as shown in Figure 14(a). However, the crystal nuclei might be easy to form at the phase boundary between PPEGA phase domains and PLA matrix (Figure 14(b)) because the surface free energy for crystal nuclei decreases due to the presence of phase boundary. On the other hand, PPEGA as a comb-like copolymer has the densely grafted PEGA chains hung on the PPEGA backbone

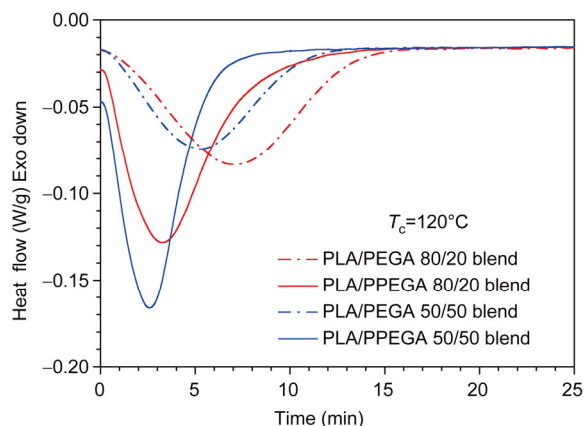


Figure 12 Heat flow curves for PLA/PEGA 80/20, PLA/PEGA 50/50, PLA/PPEGA 80/20 and PLA/PPEGA 50/50 blend samples during isothermal crystallization at T_c of 120 °C (color online).

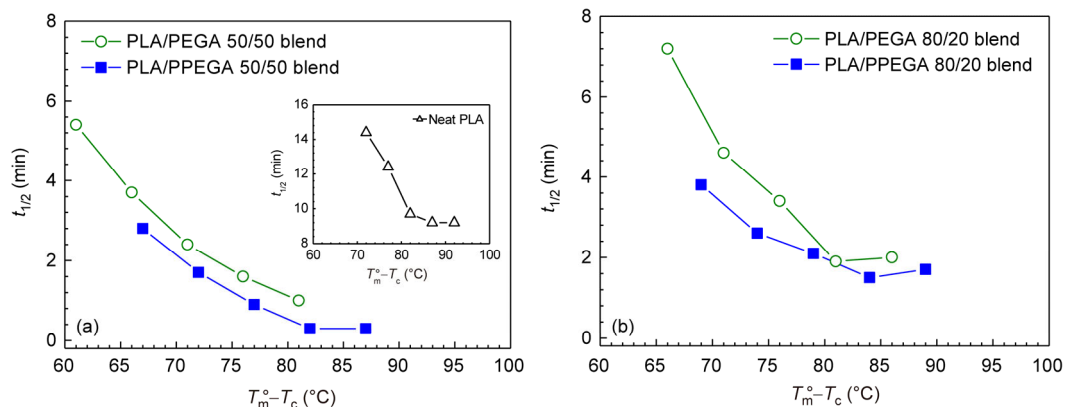


Figure 13 Changes of crystallization half-time ($t_{1/2}$) as functions of undercooling ($T_m^\circ - T_c$) for (a) neat PLA (inset), PLA/PEGA 50/50 and PLA/PPEGA 50/50 blend samples, and (b) PLA/PEGA 80/20 and PLA/PPEGA 80/20 blend samples.

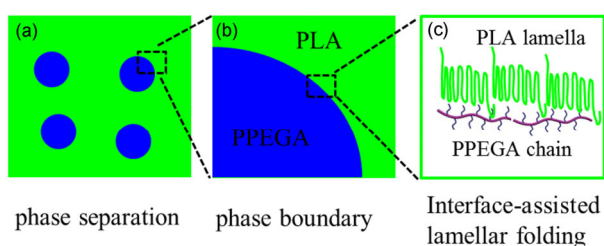


Figure 14 Schematic for illustration of interface-assisted PLA lamellar folding in PLA/PPEGA blends. (a) Phase morphology with PPEGA phase domains dispersed in PLA matrix; (b) enlarged portion showing the phase boundary between PLA and PPEGA phases; (c) formation of PLA lamella with assistance of PPEGA chain at interface (color online).

chain (Figure 14(c)) and this type of chain architecture might make the densely grafted PEGA chains take functions together at the phase boundary to simultaneously enhance the PLA chain segmental mobility through the local interfacial interactions. Through this specific function, PPEGA can accomplish the goal of interface-assisted PLA lamellar folding and increase the spherulitic growth rate (Figure 14(c)). We emphasize that PPEGA in the blends does not obviously decrease the glass transition temperature of PLA, which is an advantage for PLA material applications. Therefore, the unique PLA/PPEGA blend system in this study provides an effective way to overcome the disadvantages of PLA component, such as the slow crystallization rate in film processing and the reduction in heat resistance if blending with some miscible components (with lower T_g) for improving the crystallization rate.

4 Conclusions

The miscible blends of polylactide (PLA) and poly(ethylene glycol) methyl ether acrylate (PEGA) (PLA/PEGA blends) and immiscible blends of PLA and poly[poly(ethylene glycol) methyl ether acrylate] (PPEGA, comb-like copolymer) (PLA/PPEGA blends) are comparably investigated focusing

on the miscibility effects on the crystallization kinetics (nucleation and spherulitic growth rates) of PLA in these two different types of blends. It is quite interesting to find out that both PEGA and PPEGA components can enhance PLA spherulitic growth rates, even though PPEGA component is immiscible with PLA component. An additional advantage is that the immiscible PPEGA component dispersed in the PLA matrix can serve as the nucleating agent to enhance the nucleation density for PLA crystallization. The enhancement effect on the crystallization kinetics by addition of PPEGA component is thought to function through the local interfacial interactions between the densely grafted PEGA chains in PPEGA and PLA chains, even though the whole blend system behaves as an immiscible one. The enhanced nucleation density, increased spherulitic growth rate and remained glass transition temperature for PLA component in this type of immiscible blends promise some potential applications for preparing PLA or other polymer materials with highly performed mechanical properties such as the high heat resistance and high tensile modulus.

Acknowledgments This work was supported by the National Basic Research Program of China (2012CB025901), the National Natural Science Foundation of China (21174139), and the Open Research Fund of State Key Laboratory of Polymer Physics and Chemistry, Changchun Institute of Applied Chemistry, Chinese Academy of Sciences.

Conflict of interest The authors declare that they have no conflict of interest.

Supporting information The supporting information is available online at <http://chem.scichina.com> and <http://link.springer.com/journal/11426>. The supporting materials are published as submitted, without typesetting or editing. The responsibility for scientific accuracy and content remains entirely with the authors.

- 1 Tsarevsky NV, Matyjaszewski K. *Chem Rev*, 2007, 107: 2270–2299
- 2 Stavber G, Malic B, Kosec M. *Green Chem*, 2011, 13: 1303–1310
- 3 Ma QQ, Liu XQ, Zhang RY, Zhu J, Jiang YH. *Green Chem*, 2013, 15: 1300–1310
- 4 Renouf-Glauser AC, Rose J, Farrar DF, Cameron RE. *Biomaterials*, 2005, 26: 5771–5782

- 5 Xu H, Xie L, Jiang X, Hakkarainen M, Chen JB, Zhong GJ, Li ZM. *Biomacromolecules*, 2014, 15: 1676–1686
- 6 Wei XF, Bao RY, Cao ZQ, Yang W, Xie BH, Yang MB. *Macromolecules*, 2014, 47: 1439–1448
- 7 Saeidlou S, Huneault MA, Li HB, Park CB. *Prog Polym Sci*, 2012, 37: 1657–1677
- 8 Miyata T, Masuko T. *Polymer*, 1997, 38: 4003–4009
- 9 Robertson ML, Paxton JM, Hillmyer MA. *ACS Appl Mater Interfaces*, 2011, 3: 3402–3410
- 10 Bitinis N, Sanz A, Nogales A, Verdejo R, Lopez-Manchado MA, Ezquerro TA. *Soft Matter*, 2012, 8: 8990–8997
- 11 Fang HG, Jiang F, Wu QH, Ding YS, Wang ZG. *ACS Appl Mater Inter*, 2014, 6: 13552–13563
- 12 Lee I, Panthani TR, Bates FS. *Macromolecules*, 2013, 46: 7387–7398
- 13 Zhang YQ, Fang HG, Wang ZK, Tang M, Wang ZG. *Cryst Eng Comm*, 2014, 16: 1026–1037
- 14 Zhang YQ, Jiang F, Wang WT, Wang ZG. *J Phys Chem B*, 2014, 118: 9112–9117
- 15 Xu H, Xie L, Jiang X, Li XJ, Li Y, Zhang ZJ, Zhong GJ, Li ZM. *J Phys Chem B*, 2013, 118: 812–823
- 16 Rahman N, Kawai T, Matsuba G, Nishida K, Kanaya T, Watanabe H, Okamoto H, Kato M, Usuki A, Matsuda M, Nakajima K, Honma N. *Macromolecules*, 2009, 42: 4739–4745
- 17 Kuo SW, Huang WJ, Huang CF, Chan SC, Chang FC. *Macromolecules*, 2004, 37: 4164–4173
- 18 Neelakandan C, Kyu T. *J Phys Chem B*, 2009, 113: 8520–8526
- 19 Zhang YQ, Wang ZK, Jiang F, Bai J, Wang ZG. *Soft Matter*, 2013, 9: 5771–5778
- 20 Talibuddin S, Wu L, Runt J, Lin JS. *Macromolecules*, 1996, 29: 7527–7535
- 21 Di Lorenzo ML. *Prog Polym Sci*, 2003, 28: 663–689
- 22 Yang JM, Chen HL, You JW, Hwang JC. *Polym J*, 1997, 29: 657–662
- 23 Zhang YQ, Xu HJ, Yang JJ, Chen SY, Ding YS, Wang ZG. *J Phys Chem C*, 2013, 117: 5882–5893
- 24 Hu Y, Hu YS, Topolkaev V, Hiltner A, Baer E. *Polymer*, 2003, 44: 5711–5720
- 25 Hu Y, Hu YS, Topolkaev V, Hiltner A, Baer E. *Polymer*, 2003, 44: 5681–5689
- 26 Silvestre C, Cimmino S, Di Pace E, Martuscelli E, Monaco M, Buzarovska A, Koseva S. *Polym Networks Blends*, 1996, 6: 73–80
- 27 Avella M, Martuscelli E, Orsello G, Raimo M, Pascucci B. *Polymer*, 1997, 38: 6135–6143
- 28 Martuscelli E. *Polym Eng Sci*, 1984, 24: 563–586
- 29 Yokoyama Y, Ricco T. *J Appl Polym Sci*, 1997, 66: 1007–1014
- 30 Greco P, Martuscelli E. *Polymer*, 1989, 30: 1475–1483
- 31 Cimmino S, Dipace E, Martuscelli E, Silvestre C, Buzarovska A, Slobodanka K. *Polym Netw Blend*, 1995, 5: 63–68
- 32 Marentette JM, Brown GR. *Polymer*, 1998, 39: 1415–1427
- 33 Cascone E, David DJ, Di Lorenzo ML, Karasz FE, Macknight WJ, Martuscelli E, Raimo M. *J Appl Polym Sci*, 2001, 82: 2934–2946
- 34 Sakai F, Nishikawa K, Inoue Y, Yazawa K. *Macromolecules*, 2009, 42: 8335–8342
- 35 Zhang YQ, Xu ZH, Wang ZK, Ding YS, Wang ZG. *RSC Adv*, 2014, 4: 20582–20591
- 36 Talibuddin S, Bunt J, Liu LZ, Chu B. *Macromolecules*, 1998, 31: 1627–1634
- 37 Hoffman JD, Weeks JJ. *J Res Nat Bureau Stand Section A-Phys Chem*, 1962, 66: 13–28
- 38 Ikehara T, Kurihara H, Qiu ZB, Nishi T. *Macromolecules*, 2007, 40: 8726–8730
- 39 Xu ZH, Niu YH, Yang L, Xie WY, Li H, Gan ZH, Wang ZG. *Polymer*, 2010, 51: 730–737
- 40 Wang ZG, Hsiao BS, Sauer BB, Kampert WG. *Polymer*, 1999, 40: 4615–4627
- 41 Zhang XH, Wang ZG, Dong X, Wang DJ, Han CC. *J Chem Phys*, 2006, 125: 024907
- 42 Tsuburaya M, Saito H. *Polymer*, 2004, 45: 1027–1032
- 43 Bartczak Z, Galeski A, Krasnikova NP. *Polymer*, 1987, 28: 1627–1634
- 44 Fang HG, Zhang YQ, Bai J, Wang ZG. *Macromolecules*, 2013, 46: 6555–6565
- 45 Shao W, Zhang YQ, Wang ZG, Niu YH, Yue RJ, Hu WP. *Ind Eng Chem Res*, 2012, 51: 15953–15961
- 46 Qiu JS, Xing CY, Cao XJ, Wang HT, Wang L, Zhao LP, Li YJ. *Macromolecules*, 2013, 46: 5806–5814
- 47 Du J, Niu H, Dong JY, Dong X, Wang D, He A, Han CC. *Macromolecules*, 2008, 41: 1421–1429
- 48 Graham PD, McHugh AJ. *Macromolecules*, 1998, 31: 2565–2568
- 49 Zhao JC, Wang ZG, Niu YH, Hsiao BS, Piccarolo S. *J Phys Chem B*, 2012, 116: 147–153
- 50 Xu ZH, Niu YH, Wang ZG, Li H, Yang L, Qiu J, Wang H. *ACS Appl Mater Inter*, 2011, 3: 3744–3753